

## New occurrences of kimberlite-like intrusive rocks in drillcore from south of Wekusko Lake, eastern Flin Flon belt, north-central Manitoba (NTS 63J12)

by A.R. Chakhmouradian<sup>1</sup> and K.D. Reid

<sup>1</sup> Department of Geological Sciences, University of Manitoba, 125 Dysart Road, Winnipeg, MB

### In Brief:

- Narrow, porphyritic, carbonate-rich dikes cut Paleoproterozoic rocks south of Wekusko Lake
- Mineralogy includes macrocryst and groundmass dolomite, phlogopite, spinel and ilmenite
- Preliminary data indicate hypabyssal kimberlite, rather than magnesiocarbonatite

### Citation:

Chakhmouradian, A.R. and Reid, K.D. 2017: New occurrences of kimberlite-like intrusive rocks in drillcore from south of Wekusko Lake, eastern Flin Flon belt, north-central Manitoba (NTS 63J12); *in* Report of Activities 2017, Manitoba Growth, Enterprise and Trade, Manitoba Geological Survey, p. 78–90.

### Summary

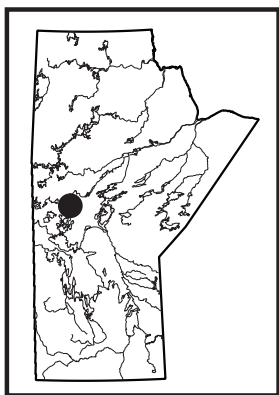
Two exploration drillholes that penetrate Precambrian basement rocks beneath the Phanerozoic limestone cover south of Wekusko Lake contain narrow but macroscopically distinguishable intercepts of dolomite-phlogopite-bearing intrusive dikes that crosscut the Paleoproterozoic rocks. These intrusive rocks were recognized during re-examination of the drillcore by the Manitoba Geological Survey during the 2016 and 2017 field seasons as part of a broader project to develop a series of 1:50 000 scale maps for the eastern portion of the sub-Phanerozoic Flin Flon belt. Both dike occurrences contain brownish-grey, predominantly inequigranular rocks that are macroscopically similar to kimberlite. Textures in the dikes vary from macrocrystic and composed of subrounded phlogopite ( $\pm$ serpentinized olivine) crystals set in a fine- to medium-grained dolomitic groundmass, to relatively equigranular, to quasi-globular owing to the presence of abundant ovoid, polygonal and irregularly shaped dolomitic aggregates. The modal composition of both dikes is broadly similar to magnesiocarbonatite previously described in the southwest corner of Wekusko Lake, but the trace-element data show greater similarity to hypabyssal kimberlite.

Presented in this report are the geological setting, drillcore observations and preliminary compositional data for dolomite, phlogopite, spinel and ilmenite from the dike sampled in 2016. Detailed petrographic and mineralogical work on the samples collected in 2017 is currently underway. If these occurrences of ‘kimberlite-like’ intrusive rocks are genetically related to the magnesiocarbonatite found in the southwest corner of Wekusko Lake, the area of mantle magmatism in the Flin Flon belt may be extended to at least 50 km<sup>2</sup>. Implications of these new findings for diamond exploration are discussed.

### Introduction

From a statistical perspective, Manitoba is relatively well endowed with respect to the number of known carbonatite occurrences, although examples of kimberlite remain elusive. Archean examples of carbonatite include those in the Oxford Lake and Knee Lake areas (Anderson et al., 2012; Anderson, 2016) and Paleoproterozoic examples were found at Eden Lake in the Trans-Hudson orogen and Paint Lake in the Superior boundary zone (Mumin, 2002; Chakhmouradian et al., 2008, 2009a; Couëslan, 2008). Carbonatite magmas are rare but known to produce significant economic concentrations of rare-earth elements, niobium and zirconium (e.g., Chakhmouradian and Wall, 2012; Chakhmouradian et al., 2015; Smith et al., 2015). In some cases, they contain more common metals, including copper, iron and molybdenum, such as at Palabora in South Africa (Aldous, 1986), Kovdor in Russia (Krasnova et al., 2004) and Huanglongpu in China (Xu et al., 2010).

The rich mining history of copper-zinc ( $\pm$ gold $\pm$ silver) volcanogenic massive sulphide (VMS) deposits in the Flin Flon belt (FFB) has resulted in exploration efforts in the region being focused heavily on its base-metal potential. Thus, it is not surprising that mantle-derived rocks of alkaline affinity were first intersected in the FFB by Falconbridge Nickel Mines Ltd. in 1983 during drill testing of the Copper-Man VMS deposit in the southwest corner of Wekusko Lake (Figure GS2017-8-1). Further drilling by European Ventures Inc. in the same location intersected what was described as a “kimberlitic rock” and reported to contain G10, G9 and possible eclogitic garnets, indicative of diamond potential. It is noteworthy that kimberlite and other carbonate-rich mantle-derived rocks (e.g., carbonatites and ultramafic lamprophyres) cannot be distinguished reliably based on their textural characteristics, but require a detailed geochemical and mineralogical analysis for their identification. A detailed petrographic study of the samples from the Falconbridge and European Ventures drillholes was undertaken by Chakhmouradian et al. (2009b) in order to identify these rocks and examine their affinity to various types of mantle-derived CO<sub>2</sub>-rich magma. Their findings were that the mineralogy and geochemistry of the studied samples were inconsistent



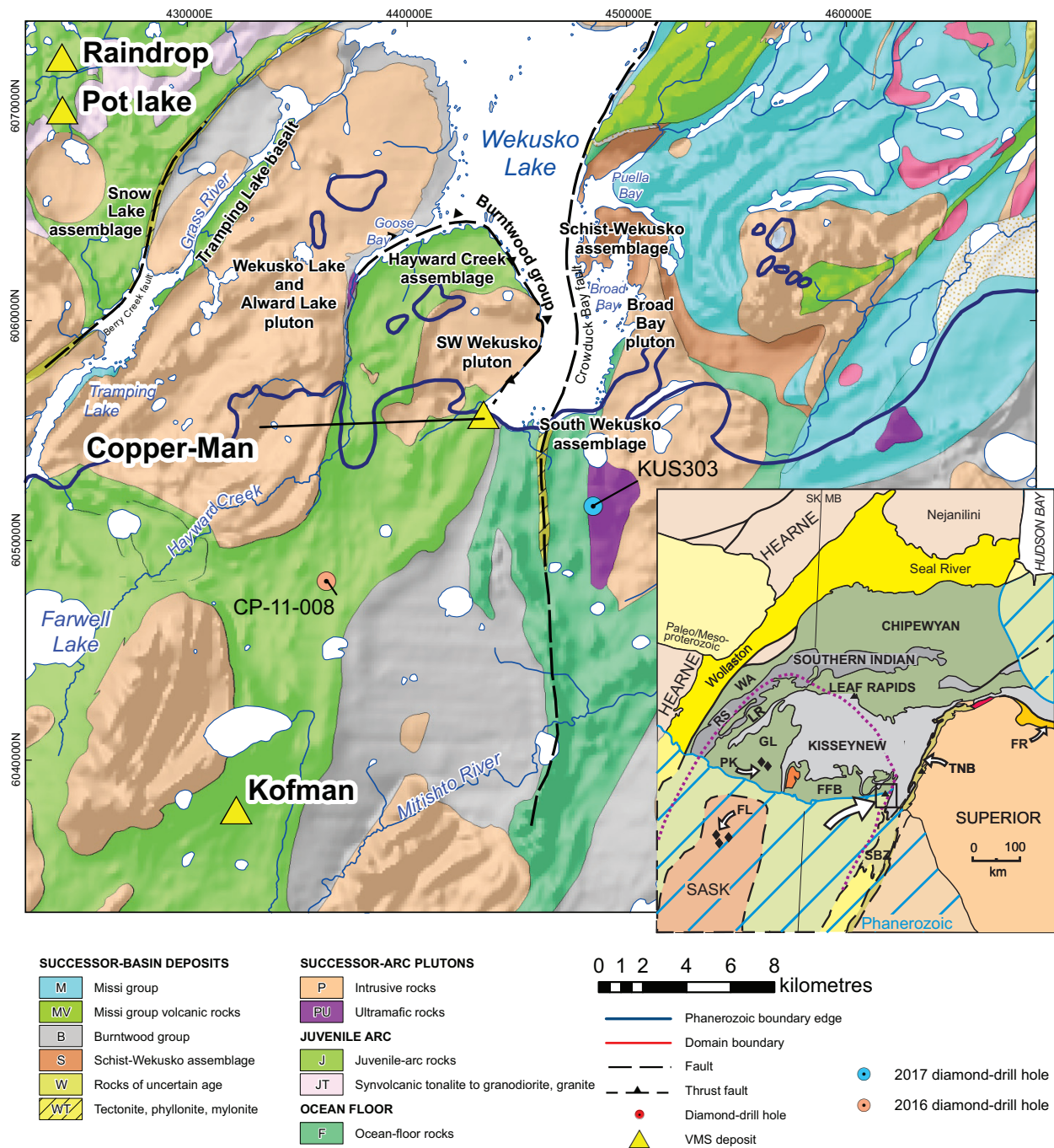


**Figure GS2017-8-1:** Geology of the south Wekusko Lake area (modified from NATMAP Shield Margin Project Working Group, 1998), showing the Copper-Man VMS deposit, where magnesiocarbonatite has been identified in drillholes GBO-16 (Assessment file 73676) and EPV-12a (Chakmouradian et al., 2009a, b; Assessment file 70569), and two new occurrences of texturally similar intrusive rocks in drillholes CP-11-008 (Assessment File 63J1159) and KUS303 (Assessment File 74423). **Inset** (modified after Zwanzig and Bailes, 2010): large white arrow shows location of south Wekusko Lake area in the Flin Flon belt (FFB) and its relation to the Kisseynew domain (KD), Superior boundary zone (SBZ), Thompson nickel belt (TNB), Fox River belt (FR), Glennie complex (GL), La Ronge belt (LR), Rottenstone domain (RS), Wathaman batholith (WA) and sub-Phanerozoic Sask craton (SASK). Fort à la Corne (FL) and Pikoo (PK) kimberlite fields indicated by diamond symbols, and triangles show Paleoproterozoic and younger carbonatite occurrences. Purple dashed line shows possible extent of Sask Craton in the lower crust.

with kimberlite. Given the modal, isotopic and trace-element composition, Chakhmouradian et al. (2009b) interpreted these rocks as primary dolomite carbonatite contaminated by mantle material (including diamond-indicator minerals) and isotopically re-equilibrated with low-temperature crustal fluids. Recent re-examination of drillcore from the area south of Wekusko Lake has identified two new occurrences of inequigranular rock that is superficially similar to kimberlite and comprises largely the same minerals as those found in the dikes near the Copper-Man VMS deposit.

## Geological setting

Wekusko Lake is at the eastern end of the FFB in the Reindeer zone of the Paleoproterozoic Trans-Hudson orogen (Lewry and Collerson, 1990). The FFB is a series of oceanic tectonostratigraphic assemblages structurally juxtaposed during intraoceanic accretion, intruded by successive arc-magma series and ultimately entrained during terminal collision of the Hearne, Superior and Sask cratons (e.g., Lucas et al., 1996; Syme et al., 1999; Hajnal et al., 2005). The belt is flanked to the north by metasedimentary gneisses of the Kisseynew domain and to the east by the Superior boundary zone, and to the south is covered by Phanerozoic sedimentary rocks (Figure GS2017-8-1).

The exposed geology of the southern section of Wekusko Lake was mapped by Gilbert and Bailes (2005) at 1:20 000 scale. Their work outlined five tectonostratigraphic blocks, from west to east the: 1) Hayward Creek assemblage of juvenile-arc affinity; 2) Burntwood Group turbidites; 3) South Wekusko assemblage of ocean-floor affinity; 4) Schist-Wekusko assemblage of successor-arc affinity; and 5) Missi group sandstone and conglomerate (see Figure GS2017-8-1). These are crosscut by multiple large intrusions of 'successor-arc' age.

The Crowduck Bay fault is a crustal-scale fault that can be traced to the north of Broad Bay before trending northeast in Crowduck Bay (not shown on Figure GS2017-8-1); it separates the Burntwood Group turbidites (2) from the South Wekusko ocean-floor basalt (3) to the east (Figure GS2017-8-1). At the south end of Wekusko Lake, the Crowduck Bay fault is traced as chlorite-carbonate schist before disappearing beneath the Phanerozoic cover (Figure GS2017-8-1).

## Kimberlite-like intrusive rocks in drillcore

### *Drillhole CP-11-008*

Drillhole CP-11-008 (Assessment File 63J1159) intersects predominantly heterolithic lapilli tuff with an overall dacitic composition. This unit is distinctive in that it contains ~5% quartz phenocrysts and 5–10% dark green, flattened mafic fragments. It then grades into a 50 m thick package comprising feldspathic wacke before grading back into dacitic feldspar-crystal tuff (Reid and Gagné, 2016). Overall the volcanoclastic rocks are moderately strained with a well-developed penetrative fabric.

Between depths of 307.75 and 308.10 m, the feldspar-crystal tuff is cut by a heterogeneous intrusive rock that varies in colour from buff brown to brownish grey (Figure GS2017-8-2a);

the lateral extent of this intrusive rock is unknown and, for discussion purposes, it is referred to as a dike. Although material along the contacts with the wallrock is not well preserved, it is evident that both contacts are sharp and associated with brittle fracturing and cryptic alteration that extends approximately 1 cm into the adjacent wallrock (Figure GS2017-8-2b). The intrusive rock is texturally heterogeneous due to the presence of layering (flow banding?) and exotic xenoliths. Figure GS2017-8-2c shows a dolomite-rich layer that contains ovoid segregations of fine-grained dolomite 1–2 mm across and is in sharp contact with a darker grey layer that contains medium- to coarse-grained phlogopite macrocrysts in an aphanitic oxide-dolomite groundmass. Figure GS2017-8-2d shows a sharp but irregular lower contact between the darker grey macrocryst-rich domain and the lower dolomite-rich domain that contains several abraded xenoliths of biotite schist. A distinct, large (~4 cm) angular xenolith of mica schist occurs in a phlogopite-dolomite-rich material close to the lower contact (Figure GS2017-8-2e). Portions of the intrusive rock are texturally similar to some material from Wekusko Lake (drillhole EPV-12a) and many hypabyssal kimberlites (e.g., Wemindji in Quebec; Zurevinski and Mitchell, 2011).

### *Drillhole KUS303*

The predominant rock type in drillhole KUS303 (Assessment File 74423) is dark green, fine-grained basalt with subordinate (<1.5 m in apparent thickness) intrusive rocks of intermediate to felsic composition, mafic wacke, finely laminated siliceous chert, and grunerite-bearing iron formation. Near the end of the drillhole, between depths of 215 and 230 m, a number of centimetre- to decimetre-scale ductile shear structures are present, and the rock type changes from basalt to gabbro (Reid, GS2017-7, this volume). Intruding a portion of the ductile shear zone is an approximately 2 m thick (227–229 m) interval of fine- to medium-grained, brownish-grey, dolomite-rich rocks that contain 5–10 vol. % orange-brown (altered?) phlogopite macrocrysts measuring up to 1.5 cm in diameter (Figure GS2017-8-3a). This interval is bounded by intensely fractured rock hosting abundant calcite- and dolomite-filled fractures. A 20 cm interval above the main intercept shows very poorly preserved intrusive material separated from the wallrock by a sharp but diffuse contact over a distance of several millimetres (Figure GS2017-8-3b). The upper contact of the main intercept is brecciated (at 226.95 m), with angular chlorite schist wallrock fragments surrounded by minor fine-grained intrusive matrix (Figure GS2017-8-3c).

Farther downhole (at 227.0 m), the brecciated rock varies from clast to matrix supported, with dark grey subangular schist fragments and late carbonate-filled fractures, the latter of which cut both wallrock and fine-grained intrusive rock (Figure GS2017-8-3d). The distribution of phlogopite macrocrysts is heterogeneous throughout the intercept, with 0.5–1.5 cm subangular to amoeboid grains of orange-brown colour concentrated at 227.1 m and, to a lesser extent, elsewhere (Figure GS2017-8-3e). At 227.7 m, the intrusive rock is characterized by a relatively equigranular groundmass hosting 0.5–2.0 mm

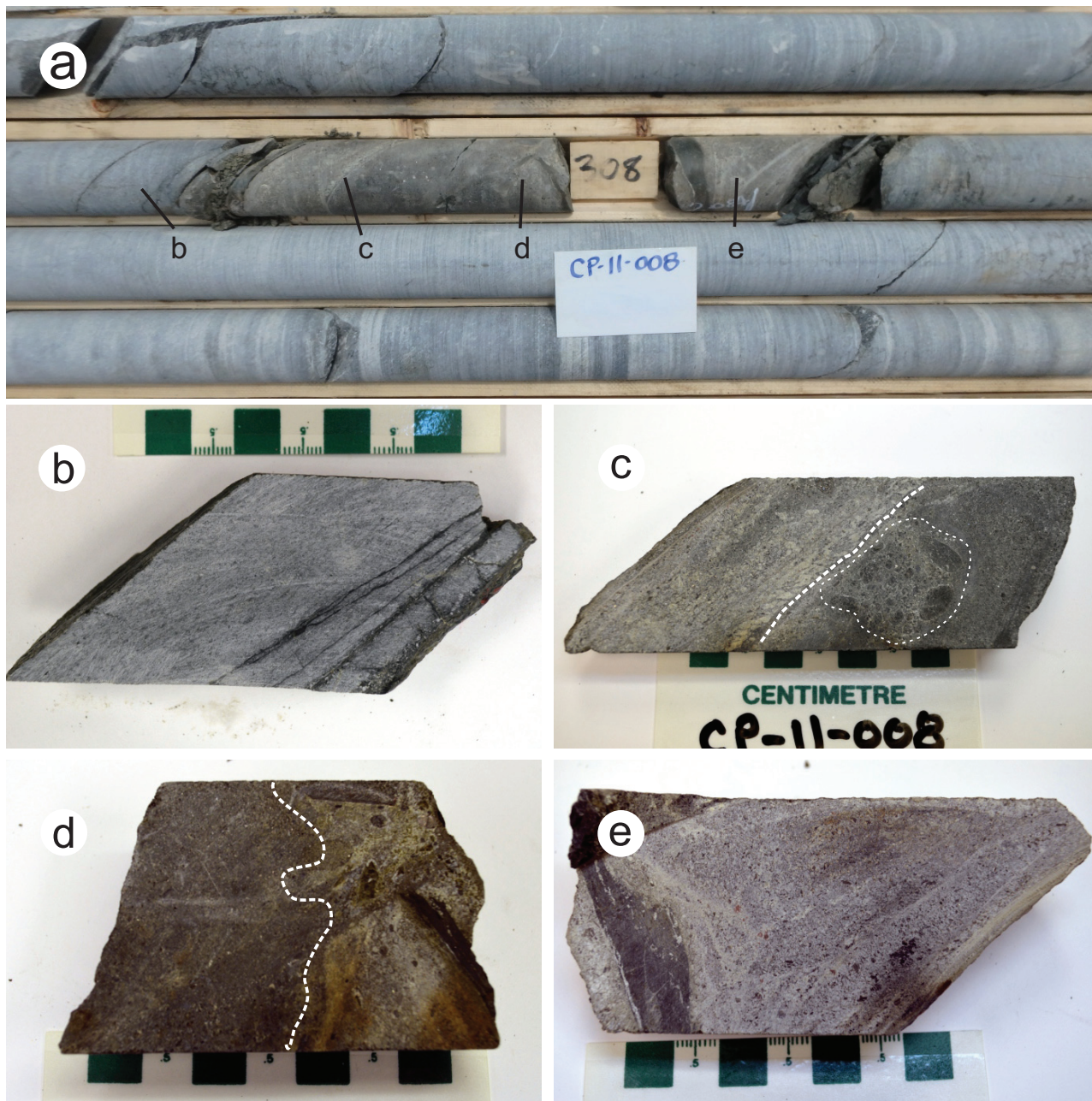


**Figure GS2017-8-2:** Drillcore photos from drillhole CP-11-008 (Assessment File 63J1159): **a)** brownish-grey intrusive rock with sharp contacts, 307.75–308.10 m; letters show the location of close-up photos; **b)** sharp upper contact between felsic lapilli tuff and the intrusive rock, 307.70–307.75 m; **c)** internal structural heterogeneity of the intrusive rock, defined by layers rich in dolomite segregations (white dashed line), phlogopite macrocrysts (circular white dashed lines) and xenoliths, 307.75–307.90 m; **d)** sharp but irregular contact (dashed white line) between darker grey phlogopite-rich and dolomite-rich layers near the lower contact, 307.90–308.00 m; **e)** large mica schist xenolith in equigranular dolomite-phlogopite layer, 308.00–308.10 m. Core is NQ diameter (4.76 cm).

rounded aggregates of fine-grained dolomite and minor phlogopite phenocrysts but few to no phlogopite macrocrysts (Figure GS2017-8-3f). The groundmass texture becomes more variable closer to the lower contact owing to intercalations of fine-grained phaneritic and aphanitic material (Figure GS2017-8-3g). The brown macrocryst-rich intrusive rock from drillhole KUS303 is superficially similar to altered hypabyssal kimberlite, alnoite

and other carbonate-rich mantle-derived rocks, and thus cannot be identified with any degree of confidence in the absence of detailed petrographic, geochemical and mineralogical data.

### Petrography

To date, four samples representing the upper ~25 cm of the dike intersected by drillhole CP-11-008 have undergone detailed

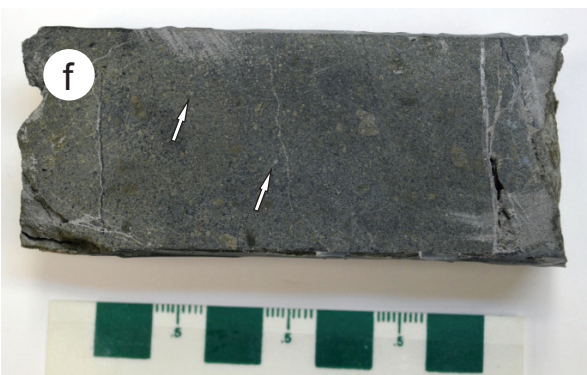
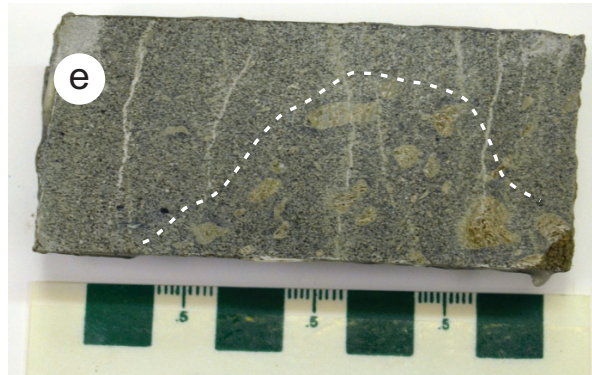
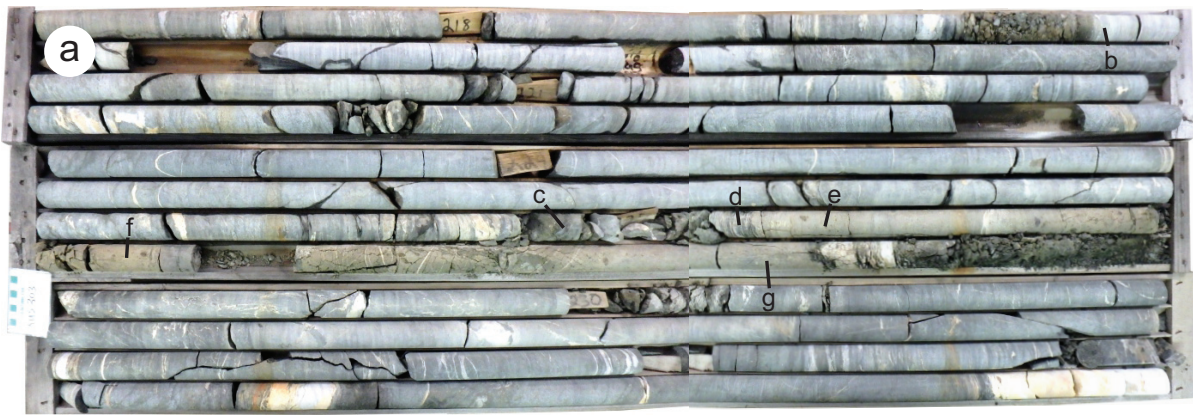


**Figure GS2017-8-3:** Drillcore photos from drillhole KUS303 (Assessment File 74423): **a)** main intrusive intercept (227–229 m); letters show the location of close-up photos; **b)** sharp but diffuse contact between the intrusive material and wallrock metadacite, 218.8 m; **c)** clast-supported, chlorite schist breccia with a carbonate matrix, 226.95 m; **d)** gradation from clast-supported to matrix-supported breccia at the intrusive rock contact, 227.0 m; arrow points to a late-stage carbonate-filled vein; **e)** locally concentrated phlogopite macrocrysts (dashed line), 227.10 m; **f)** relatively equigranular igneous material with ovoid dolomite aggregates (arrows), 227.70 m; **g)** texturally heterogeneous (possibly layered) intrusive material with grain-size variations in the groundmass, 228.55 m. Core is BQ diameter (3.65 cm).

petrographic and mineralogical study. The rock examined is remarkably heterogeneous in texture. A thin (~5 mm) selvage adjacent to the contact with the host metadacitic rock contains numerous phlogopite crystals and slender laths of dolomite up to 1 mm in length arranged at 50–90° to the contact (Figure GS2017-8-4a). The laths are ‘sheathed’ in microcrystalline granular dolomite and resemble quench textures observed in the selvages of some carbonatite dikes (e.g., Chakhmouradian et al., 2016, Figures 3c, 5c), as well as mantled microphenocrysts in some hypabyssal kimberlites (Chakhmouradian, unpublished data). In the contact zone, dolomite also occurs as ovoid aggregates of minute (20–60 µm across) polygonal grains and in the groundmass (Figure GS2017-8-4a). The groundmass also contains euhedral grains of spinel-group minerals, phlogopite and apatite surrounded by serpentine. The proportion of ovoid aggregates and phlogopite increases in abundance away from the contact, whereas dolomite laths and spinel-group minerals decrease, and the former disappear completely within 1 cm

from it. Both phlogopite plates and dolomite laths are oriented obliquely to the intrusive contact outside the selvage zone (Figure GS2017-8-4b). In addition to these morphological changes, phlogopite crystals and groundmass grains are appreciably larger in the interior of the dike relative to the selvage zone.

Dolomite aggregates, phlogopite crystals and polymineralic groundmass remain the major structural elements up to a distance of ~5 cm from the upper contact. Within this interval, the rock is crudely layered and light coloured. Three types of dolomite aggregates were identified (listed in order of decreasing abundance): ovoid, irregularly shaped and polygonal (Figure GS2017-8-4c). Both ovoid and polygonal aggregates do not exceed 1.2 mm across and are composed of fine-grained (20–60 µm across) dolomite coarsening inward (Figure GS2017-8-4d), whereas the irregularly shaped aggregates are larger (up to 3 mm across) and contain generally coarser grains (locally up to 0.6 mm across). Phlogopite occurs in the groundmass and

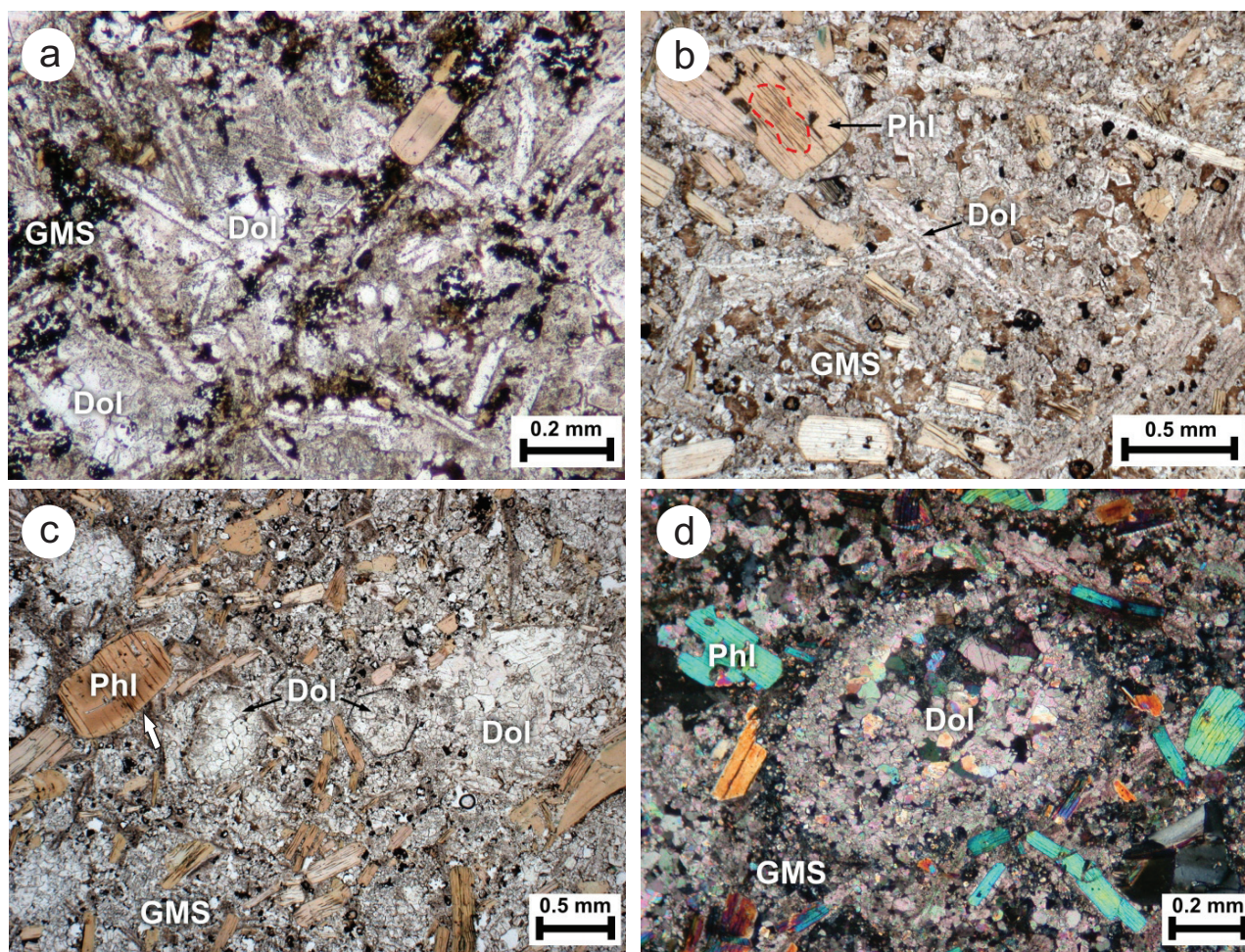


**Figure GS2017-8-4:** Thin-section photomicrographs of carbonate intrusive rock near its upper contact with metadacite (~307.8 m), drillhole CP-11-008: **a)** dolomite laths (Dol) in a groundmass (GMS) composed of granular dolomite, spinel-group minerals, phlogopite, apatite and serpentine; **b)** phlogopite crystals (Phl) and dolomite laths (Dol) oriented subparallel to the upper contact and set in a finer grained groundmass, similar to that shown in (a) but containing a lower proportion of spinel (opaque); **c)** ovoid (left), polygonal (centre) and irregularly shaped (right) dolomite (Dol) aggregates, ~1.5 cm from the upper contact; note the abundance of macrocrystic and groundmass phlogopite and a relatively small proportion of spinel in this part of the dike; **d)** characteristic concentric, granular structure of ovoid dolomite aggregate (Dol), showing an inward pattern of grain coarsening.

as thick tabular crystals up to 2 mm in length that show simple zoning and evidence of resorption, both at the core-rim boundary and along their margin (Figure GS2017-8-4c, white arrow). Because the larger tabular crystals were clearly not in equilibrium with their host melt, they will be referred to hereafter as macrocrysts rather than phenocrysts.

At a distance of ~5 cm from the contact, the rock colour changes to dark greenish grey, and its texture to massive and conspicuously inequigranular (Figure GS2017-8-2c). In this part of the dike, which extends for ~10 cm inward, the rock is composed of abundant phlogopite macrocrysts similar to those in the layered zone. However, it also contains minor chlorite, serpentine pseudomorphs after olivine (or, less likely, monticellite), phlogopite macrocrysts up to 2 mm in length (Figure GS2017-8-5a) and rounded biotite-quartz xenoliths up to 4 mm in diameter (Figure GS2017-8-5b) set in a fine-grained polymineralic groundmass. The groundmass comprises euhedral atoll-

textured spinel-group minerals, cube-shaped rutile ( $\pm$ parisite) pseudomorphs after perovskite<sup>2</sup>, hopper apatite crystals, platy phlogopite and anhedral dolomite grains set in a serpentine mesostasis (Figure GS2017-8-5c). The spinels and pseudomorphs after perovskite do not exceed 150  $\mu$ m across, whereas apatite prisms are generally much smaller (<20  $\mu$ m in diameter). Identification of the petrogenetically important accessory mineral perovskite (e.g., Reguir et al., 2010; Chakhmouradian et al., 2013), the precursor mineral to the parisite-rutile pseudomorphs, was determined from quantitative analysis of scarce unaltered cubic crystals and its Raman spectrum.

The proportions of serpentinized olivine and biotite-quartz xenoliths vary appreciably across the massive zone, whereas macrocrystic phlogopite is distributed relatively uniformly but exhibits an increasing degree of chloritization toward the centre of the intrusive interval. The central zone is texturally heterogeneous owing to the presence of randomly oriented crustal

<sup>2</sup> Parisite is a fluorocarbonate of light rare-earth elements with the general formula  $\text{CaREE}_2(\text{CO}_3)_3\text{F}_2$ ; perovskite is a complex oxide mineral with the formula  $(\text{Ca},\text{Na},\text{REE})(\text{Ti},\text{Nb},\text{Fe})\text{O}_3$ .

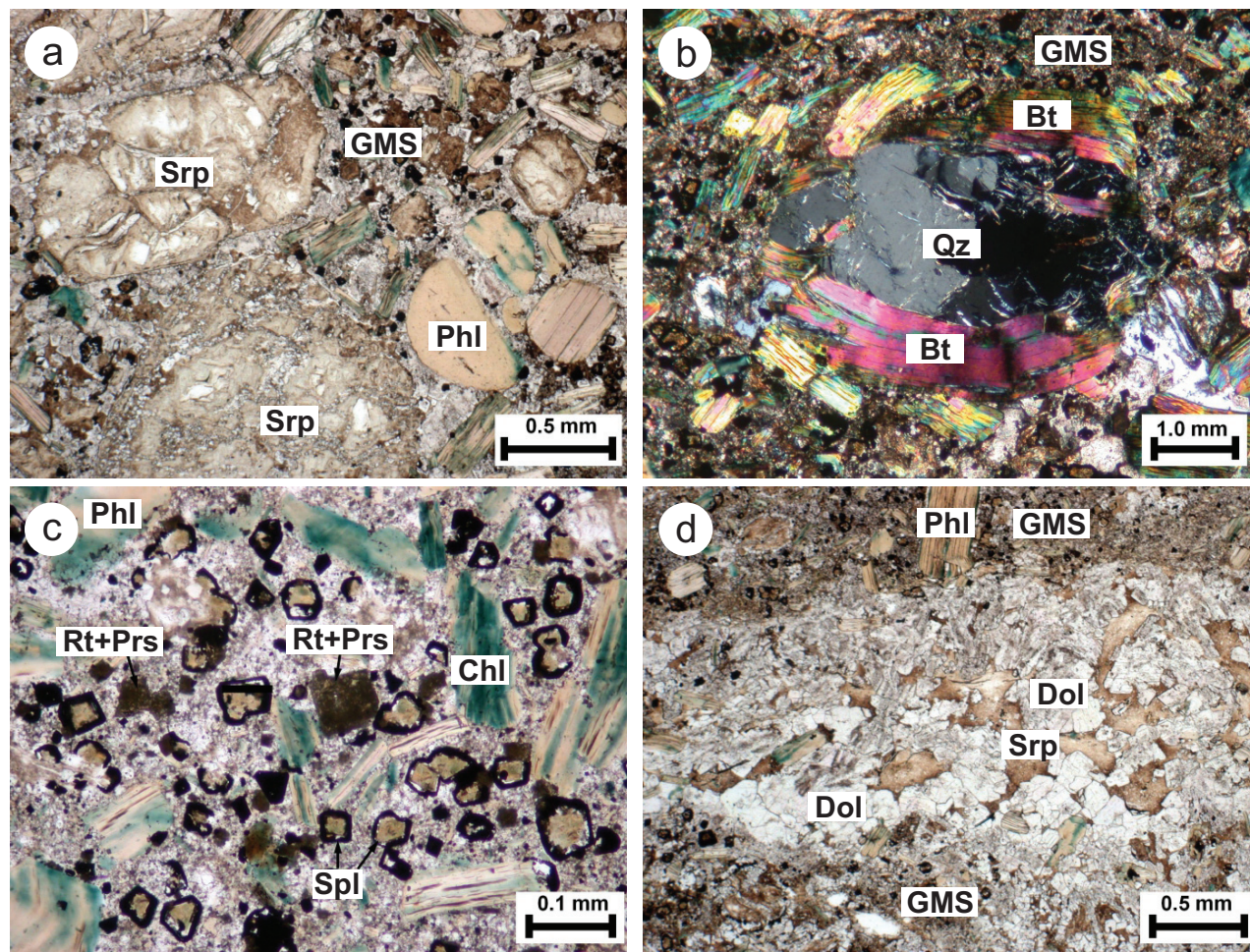


**Figure GS2017-8-5:** Thin-section photomicrographs of carbonate intrusive rock near its axial zone (~308 m), drillhole CP-11-008: **a)** serpentinized macrocrysts of olivine or monticellite (Srp) and phlogopite (Phl) macrocrysts set in a groundmass (GMS) of dolomite, phlogopite, serpentine and opaque phases; **b)** rounded xenolith composed of quartz (Qz) and biotite (Bt); **c)** rutile-parisite (Rt+Prs) pseudomorphs after perovskite, atoll-textured spinel crystals (Sp) and partially chloritized (Chl) phlogopite (Phl) in the groundmass; **d)** lenticular aggregate of euhedral dolomite (Dol) crystals with interstitial serpentine (Srp); note grain-size contrast relative to the adjacent groundmass (GMS).

xenoliths (some as large as 4 cm), domains enriched in dolomite aggregates and those enriched in serpentinized olivine. Texturally, this zone is characterized by the presence of 1) elongate light-coloured patches composed of coarser grained (relative to the surrounding groundmass) euhedral dolomite and occasional chloritized phlogopite set in a serpentine mesostasis (Figure GS2017-8-5d); 2) dolomite mantles around serpentinized olivine; and 3) relatively coarse (up to 1 mm across), zoned dolomite grains in the groundmass. The remainder of the groundmass is similar to that in the massive zone (i.e., comprises atoll-textured spinel-group minerals, rutile pseudomorphs after perovskite, apatite, chloritized phlogopite and serpentine).

Perhaps the most notable mineralogical feature of the dike in drillhole CP-11-008 is the abundance of opaque macrocrysts throughout the four texturally distinct zones described above. Most common are abraded ilmenite grains up to 2 mm across. Most of these macrocrysts are extremely irregular in shape and often fractured, and exhibit an embayed margin decorated with euhedral rutile-parisite pseudomorphs after perovskite; these pseudomorphs, in turn, are partially overgrown by spinel-group minerals (Figure GS2017-8-6a). The reaction-induced rim is variable in thickness and spongy, indicating the loss of some chemical components during the replacement. Notably, ilmenite was not observed in the groundmass. Spinel-group minerals occur both in the groundmass and as atoll-textured macrocrysts up to 0.6 mm across (Figure GS2017-8-6a). Some of the macrocrysts are abraded and lack an atoll-type rim. The chemical composition of these minerals is described in the next section.

## Mineral chemistry

Selected minerals from the CP-11-008 dike were analyzed for major and minor elements using a Cameca SX100 automated electron microprobe operated at an accelerating voltage of 15 kV and a beam current of 20 nA. A carefully selected set of standards and peak-measurement parameters was used in

each case to minimize matrix effects and potential peak overlaps. The empirically determined lower detection limits were <800 ppm for all elements reported here.

Dolomite is the principal constituent throughout the dike and shows great morphological diversity (see above). However, the compositions of all dolomite varieties fall within a fairly limited range (i.e.,  $\text{Dol}_{75-85}\text{Ank}_{11-24}\text{Rds}_{0-4}$ , where  $\text{Dol} = \text{CaMg}[\text{CO}_3]_2$ ,  $\text{Ank} = \text{CaFe}[\text{CO}_3]_2$  and  $\text{Rds} = \text{CaMn}[\text{CO}_3]_2$ ). The SrO content ranges from 0.1 to 0.6 wt. %, whereas Ba is below its detection limit. Of all the morphological types, zoned crystals from the centre of the dike are characterized by the greatest compositional variation, involving a decrease in their Fe content coupled with an increase in Mg, Mn and Sr from the core outward.

The C and O stable-isotope ratios were measured in dolomite from all parts of the dike that have been petrographically studied. Eight powdered samples were digested in  $\text{H}_3\text{PO}_4$  to produce  $\text{CO}_2$  gas, which was analyzed using a Finnigan Gas-Bench II on-line gas preparation and introduction system connected to a Thermo Finnigan Delta V Plus isotope-ratio mass spectrometer. Calibration was performed by analyzing two international calcite standards at the beginning, middle and end of each sample run. For quality check, calibrated internal calcite and dolomite standards were analyzed simultaneously with the samples. Multiple analyses of these standards yielded results within the standard deviation from the reference values ( $\pm 0.10\text{‰}$  for  $\delta^{13}\text{C}_{\text{V-PDB}}$  and  $\pm 0.15\text{‰}$  for  $\delta^{18}\text{O}_{\text{V-SMOW}}$ ). The measured isotope ratios show very limited variation that cannot be correlated with any specific morphological type of dolomite ( $\delta^{13}\text{C}_{\text{V-PDB}} = -3.8$  to  $-4.0\text{‰}$ ;  $\delta^{18}\text{O}_{\text{V-SMOW}} = 19.5$  to  $22.2\text{‰}$ ) and are therefore consistent with the electron-microprobe results.

Mica crystals show an extensive compositional variation and form two discrete populations on element-correlation diagrams. The darker coloured cores of some strongly zoned macrocrysts are biotite characterized by low mg# (molar  $\text{Mg}/[\text{Mg}+\text{Fe}]$ ), ranging between 0.32 and 0.49, low Ti (1.4–2.5 wt. %

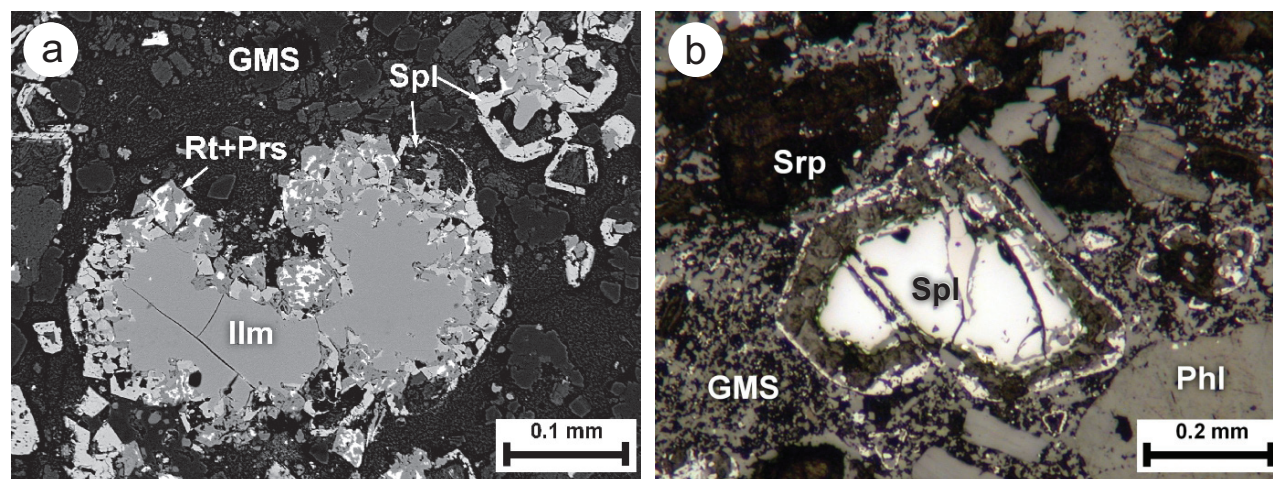


**Figure GS2017-8-6:** Morphology of mantle-indicator minerals from the carbonate intrusive rock intersected by drillhole CP-11-008: **a)** backscattered-electron scanning electron microscope image of heavily resorbed ilmenite (Ilm) macrocrysts that are discontinuously overgrown by perovskite, now completely replaced by 'spongy' rutile-parisite (Rt+Prs) pseudomorphs and spinel (Spl); **b)** atoll-textured spinel (Spl) macrocryst set in apatite-serpentine-phlogopite-dolomite groundmass (GMS).

TiO<sub>2</sub>) and absence of detectable Cr. Macrocryst rims and groundmass grains define a single phlogopite population enriched in Mg (mg# = 0.70–0.78), Ti and Cr (up to 3.5 and 0.7 wt. % of the respective oxides). Individual zoned macrocrysts show a rimward increase in Fe coupled with a decrease in Cr and Ti.

Ilmenite macrocrysts are devoid of zoning and high in Mg and Cr (10.4–12.5 and up to 6.5 wt. % of the respective oxides; Figure GS2017-8-7a) but poor in Mn (0.2–0.5 wt. %

MnO). Notably, all analyzed grains also contain detectable Al (0.3–0.5 wt. % Al<sub>2</sub>O<sub>3</sub>), which is rarely reported in published electron-microprobe data for ilmenite. The measured compositions show a somewhat lower-than-expected TiO<sub>2</sub> content (Figure GS2017-8-7b), owing to the presence of Fe<sup>3+</sup> substituting for Ti in ilmenite. The formulae calculated on a stoichiometric basis (two cations and three oxygen atoms) give between 4 and 7 mol. % Fe<sub>2</sub>O<sub>3</sub> (i.e., are lower than the Fe<sub>2</sub>O<sub>3</sub> levels suggested

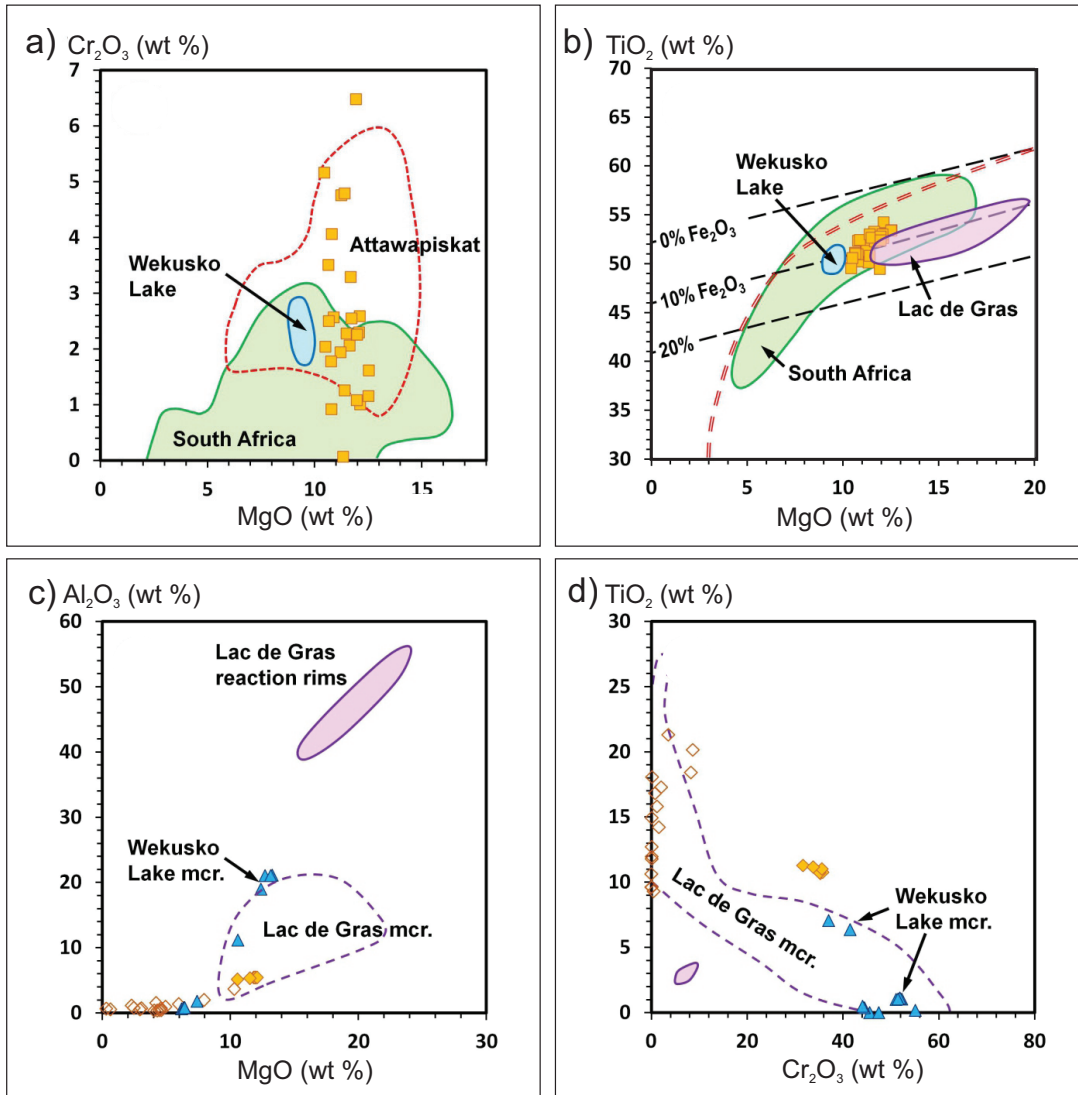


**Figure GS2017-8-7:** Compositional variation (wt. % oxides) of ilmenite and spinel-group minerals from the carbonate intrusive rock intersected by drillhole CP-11-008: **a)** MgO vs. Cr<sub>2</sub>O<sub>3</sub> in ilmenite macrocrysts from CP-11-008 (brown squares) compared to those from Wekusko Lake dolomite carbonatites (Chakhmouradian et al., 2009b), South African kimberlites (Wyatt et al., 2004) and Attawapiskat, Ontario kimberlites (Kong et al., 1999); **b)** MgO vs. TiO<sub>2</sub> in ilmenite macrocrysts from CP-11-008 (brown squares) compared to those from Wekusko Lake dolomite carbonatites (Chakhmouradian et al., 2009), South African kimberlites (Wyatt et al., 2004) and Lac de Gras, Northwest Territories kimberlites (Chakhmouradian, unpublished data); dashed lines indicate estimated Fe<sub>2</sub>O<sub>3</sub> content and double-dashed line separates fields of kimberlitic (right) and nonkimberlitic (left) ilmenite (according to Wyatt et al., 2004); **c)** MgO vs. Al<sub>2</sub>O<sub>3</sub> in macrocrysts and groundmass grains of spinel-group minerals (filled and empty diamonds, respectively) compared to macrocrysts from Wekusko Lake dolomite carbonatites (Chakhmouradian et al., 2009b) and Lac de Gras kimberlites (Chakhmouradian, unpublished data); purple field shows compositional range of reaction rims on macrocrysts from Lac de Gras kimberlites; **d)** TiO<sub>2</sub> vs. Cr<sub>2</sub>O<sub>3</sub> in macrocrysts and groundmass grains of spinel-group minerals (filled and empty diamonds, respectively) compared to macrocrysts from Wekusko Lake dolomite carbonatites (Chakhmouradian et al., 2009b) and Lac de Gras kimberlites (Chakhmouradian, unpublished data). Abbreviation: mcr., macrocrysts.

by the discrimination diagram of Wyatt et al. [2004]). The most likely reason for this discrepancy is the enrichment of the current samples in Cr and Al, which substitute for Ti in the structure and thus would account for some of the apparent Ti deficit.

Spinel macrocrysts (Figure GS2017-8-7c, d) are rich in Mg, Al, Ti and Cr (10.3–12.1, 5.2–5.5, 10.7–11.3 and 31.7–35.8 wt. % respective oxides) at low Mn levels. They can be classified as magnesiochromite (~45 mol. %  $\text{MgCr}_2\text{O}_4$ ) with significant proportions of ulvöspinel ( $\text{Fe}_2\text{TiO}_4$ ), magnetite ( $\text{FeFe}_2\text{O}_4$ ) and spinel ( $\text{MgAl}_2\text{O}_4$ ). Groundmass grains and rims on ilmenite and spinel macrocrysts correspond to Al-Cr-poor (<2.0 and 3.5 wt. % respective oxides) but relatively Mg-Ti-rich magnetite (2.3–7.9 and 9.6–21.3 wt. % respective oxides). In addition to Ti, the Mn content is also elevated in the magnetite relative to the macrocrysts (0.6–1.7 vs. 0.2–0.4 wt. % MnO, respectively).

## Geochemistry

Bulk-rock major- and trace-element data are available only for one sample (total-digestion ICP-MS; # K08914, HudBay Minerals Inc., unpublished data) from the KUS303 core (depth 228.0 m). The rock is ultrabasic and carbonate rich (all values in wt. %): 29.03%  $\text{SiO}_2$ , 2.97%  $\text{TiO}_2$ , 2.33%  $\text{Al}_2\text{O}_3$ , 23.76%  $\text{MgO}$ , 9.86%  $\text{CaO}$ , 0.21%  $\text{MnO}$ , 9.41%  $\text{FeO}_{\text{total}}$ , 0.44%  $\text{Na}_2\text{O}$ , 0.51%  $\text{K}_2\text{O}$ , 14.80%  $\text{CO}_2$ , 0.19%  $\text{P}_2\text{O}_5$ , 19.80% LOI. Of particular note are the high levels of both compatible and incompatible trace elements (e.g., 155 ppm V, 958 ppm Cr, 844 ppm Ni, 195 ppm Zr, 143 ppm Nb, 325 ppm Ba, 470 ppm REE, 23 ppm Th). The abundances of trace elements normalized to the primitive-mantle values (McDonough and Sun, 1995) are shown in Figure GS2017-8-8. Key petrogenetic ratios are as follows:  $\text{K/Sr} = 7.4$ ,  $\text{Co/Ni} = 0.11$ ,  $\text{Ga/Al} = 0.00049$ ,  $(\text{La/Yb})_{\text{CN}} = 37$ ,  $\text{Zr/Hf} = 20$ ,  $\text{Th/U} = 2.8$ ,  $\text{Nb/Ta} = 16$ .

## Discussion

Based on the currently available mineralogical and geochemical evidence, the intrusive rocks intersected in drillholes CP-11-008 and KUS303 bear a strong resemblance to the Wekusko Lake carbonatite dikes described by Chakhmouradian et al. (2009a, b). The principal similarities are 1) the extremely inequigranular nature of these rocks; 2) the presence of basement xenoliths and abundance of dolomite, phlogopite and oxide macrocrysts in their modal composition; and 3) their enrichment in Cr and REE (among other incompatible elements). Although bulk-rock data are not yet available for the CP-11-008 sample, its enrichment in Cr is clearly manifested in the compositions of phlogopite, ilmenite and spinel macrocrysts, whereas the abundance of parisite also implies high levels of REE. Dolomite from drillhole CP-11-008 is very similar to that from drillhole GBO-16 (Wekusko Lake) in its major-element and C-O stable-isotope compositions (i.e., both are low-Fe, relatively Sr-rich varieties showing low  $\delta^{13}\text{C}_{\text{V-PDB}}$  but high  $\delta^{18}\text{O}_{\text{V-SMOW}}$  values). Significant mineralogical differences, however, are observed between the Wekusko Lake dikes and the CP-11-008 samples. The latter contain serpentinized olivine, magnetite and (pseudomorphed) perovskite in the groundmass but lack zircon and apatite phenocrysts. Mineralogically, the CP-11-008 dike is more similar to hypabyssal kimberlites, and this resemblance is underscored by some of its microtextural characteristics, such as the perovskite-magnetite reaction rims on ilmenite macrocrysts,  $\text{TiO}_2$  pseudomorphs after perovskite (Chakhmouradian and Mitchell, 2000) and mantled dolomite microphenocrysts (Chakhmouradian, unpublished data).

The compositions of ilmenite and spinel macrocrysts from CP-11-008 are compared to those in the Wekusko Lake dikes and bona fide kimberlites in Figure GS2017-8-7. In terms of

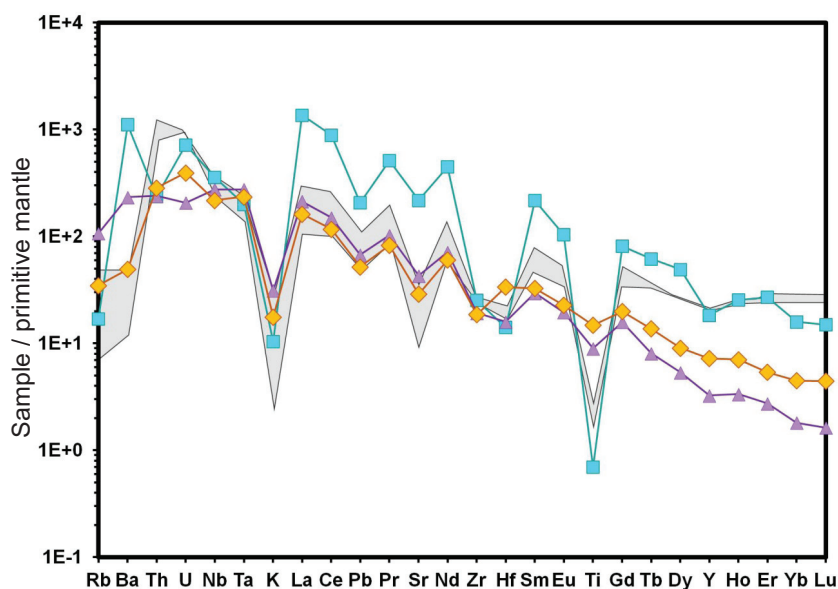


**Figure GS2017-8-8:** Chondrite-normalized trace-element profile of carbonate intrusive rock from drillhole KUS303 (yellow diamonds; normalized to the primitive-mantle values of McDonough and Sun, 1995), compared to the average profiles of hypabyssal kimberlites (purple triangles; Chakhmouradian et al., 2013) and anorogenic dolomite carbonatites (blue squares; Chakhmouradian et al., 2009b), and to the profile of the Wekusko Lake dolomite carbonatite dikes (grey field).

its Mg, Cr and Mn contents, ilmenite examined in this study is similar to macrocrysts from on-craton kimberlites worldwide. Note, however, that compositionally similar macrocrysts were also reported previously from carbonatites and carbonate-rich ultramafic lamprophyres (Chakhmouradian et al., 2009b; Tappe et al., 2009), so their presence in a mantle-derived rock cannot be used for its reliable identification. Macrocrystic spinel in kimberlites (e.g., Mitchell, 1986, 1995) and other mantle-derived carbonate-rich rocks (Tappe et al., 2006, 2009; Chakhmouradian et al., 2009b; Brady and Moore, 2012) is similar to the macrocrysts examined in this study in terms of its Mg, Al and Cr contents (comparison to Lac de Gras kimberlite spinel is shown in Figure GS2017-8-7c, d) but usually shows lower levels of Ti (<9 wt. % TiO<sub>2</sub>). Groundmass grains correspond to low-Cr-Al and high-Mg-Ti compositions, akin to the magnesioferri-rite-ulvöspinel-magnetite series characteristic of kimberlites (Mitchell, 1986, 1995).

The sample from drillhole KUS303 analyzed by HudBay Minerals is geochemically akin to kimberlites; in fact, with the exception of somewhat lower Rb and Ba abundances and higher levels of heavy REE (Gd-Lu), this rock is almost identical to the average hypabyssal kimberlite (Figure GS2017-8-8). Dolomite carbonatites are characterized by generally higher levels of divalent large-ion lithophile elements and REE (Figure GS2017-8-8). More importantly, however, carbonatites and kimberlites can be reliably distinguished on the basis of certain element ratios, which are sensitive to both the nature of mantle sources of these rocks and petrogenetic processes involved in their evolution (Chakhmouradian, 2006; Chakhmouradian et al., 2009b, 2013). In kimberlites, these indicator ratios approach primitive-mantle (and chondritic) values (e.g., K/Sr = 9 vs. 12, Co/Ni = 0.07 vs. 0.05, Nb/Ta = 18 vs. 18, respectively). In contrast, anorogenic carbonatites exhibit a very different trace-element signature (e.g., K/Sr = 0.6, Co/Ni = 2.7, Nb/Ta = 39 for dolomitic rocks), implying their derivation from an unusual mantle source or their geochemically evolved nature. The KUS303 dike shows primitive-mantle-like indicator ratios similar to those in kimberlites and no evidence of element loss through fractionation or wall-rock metasomatism.

To summarize, the currently available evidence strongly indicates that the intrusive rocks identified in drillholes CP-11-008 and KUS303 may be related to those intersected farther north beneath Wekusko Lake or, at least, are derived from a similar mantle source enriched in carbon and incompatible elements. At all three localities, the emplacement of parental magma must have been rapid enough to preserve mantle-derived indicator minerals and to facilitate the entrainment of wallrock material. The structures and textures observed in the drillcore and thin sections imply emplacement by injection into fractured basement rocks below the surface of magma fluidization. True segregation textures, such as those typifying the transitional facies of some kimberlite intrusions (Hetman et al., 2004; Skinner and Marsh, 2004), are not observed in the dikes at any of the three localities. That the level of fluidization was not reached is also consistent with the stable-isotope data, which do not indicate any significant CO<sub>2</sub> loss, as would have

occurred during magma fluidization. The stable-isotope data for both the Wekusko Lake and the CP-11-008 dikes, however, do record re-equilibration of primary igneous dolomite with a low-temperature, <sup>18</sup>O-enriched reservoir, potentially representing Lower Paleozoic seawater (for further discussion, see Chakhmouradian et al., 2009b). A detailed mineralogical and geochemical study of the newly discovered intrusive dikes is presently underway as a collaborative project between the University of Manitoba and the Manitoba Geological Survey.

## Economic considerations

Although indicator minerals such as Mg-Cr-rich ilmenite and spinel cannot be used to identify the type of magma that transported them (Mitchell et al., 1999; Chakhmouradian et al., 2009b; Tappe et al., 2009; Brady and Moore, 2012), their occurrence in the rock is an important hallmark of mantle-derived silica-undersaturated and carbonate-rich intracontinental magmatism that is known to produce diamond deposits. In this context, kimberlite is not the only type of magma that is of potential interest in diamond exploration, other notable examples being ultramafic lamprophyres and carbonatites (Mitchell et al., 1999; Dignonnet et al., 2000). As has been emphasized numerous times in the literature (e.g., Raeside and Helms-taedt, 1982; Mitchell, 1983, 1995; Reguir et al., 2009), reliable identification of (potentially) diamondiferous rocks requires a painstaking analysis of their petrography, of compositional variations exhibited by major and accessory phases, and of the whole-rock trace-element budget. With the two new localities of kimberlite-like rocks described in this report, the extent of ultrabasic, carbonate-rich magmatism in the southern Wekusko Lake area may be greater than 50 km<sup>2</sup> (Figure GS2017-8-1).

It is also noteworthy that young cryptovolcanic structures have been documented farther south, at Shoulderblade Island in South Moose Lake (Bezys and Bamburak, 1994) and at Easterville (Bezys et al., 1996). Although the data available for these localities are presently insufficient to claim any petrogenetic connection to the Wekusko area dikes, they do indicate that this part of the Trans-Hudson orogen (and underlying Sask craton: Hajnal et al., 2005) has experienced (possibly, more than once) extensional tectonic reactivation and associated magmatism since the Paleoproterozoic. Further indicator-mineral sampling and geophysical exploration are warranted along the southern margin of the FFB and into the Interlake Region to ascertain the extent of kimberlite-like magmatism in this part of Manitoba.

## Acknowledgments

The authors thank M. Stocking, C. Stocki, and S. Walker for providing enthusiastic field assistance, as well as N. Brandon and E. Anderson for thorough logistical support. Additional thanks go to C. Epp and C. Stocki for help handle of samples in the laboratory. They are grateful to HudBay Minerals Inc. and Royal Nickel Inc. for providing access and facilities to examine drillcore. The Natural Sciences and Engineering Research Council of Canada provided funding for micro-analytical analyses

through a grant to A. Chakhmouradian (University of Manitoba).

## References

- Aldous, R.T.H. 1986: Copper-rich fluid inclusions in pyroxenes from the Guide copper mine, a satellite intrusion of the Palabora igneous complex, South Africa; *Economic Geology*, v. 81, p. 143–155.
- Anderson, S.D. 2016: Preliminary results of bedrock mapping at central Knee Lake, northwestern Superior province, Manitoba (parts of NTS 53L15, 53M2); *in Report of Activities 2016, Manitoba Growth, Enterprise and Trade, Manitoba Geological Survey*, p. 1–15.
- Anderson, S.D., Kremer, P.D. and Martins, T. 2012: Preliminary results of bedrock mapping at Oxford Lake, northwestern Superior province, Manitoba (parts of NTS 53L12, 13, 63I9, 16); *in Report of Activities 2012, Manitoba Innovation, Energy, and Mines, Manitoba Geological Survey*, p. 6–22.
- Bezys, R.K. and Bamburak, J.D. 1994: Geological investigation of Shouderblade Island structure, South Moose Lake, NTS 63F16; *in Report of Activities 1994, Manitoba Energy and Mines, Minerals Division*, p. 142–143.
- Bezys, R.K., Fedikow, M.A.F. and Kjarsgaard, B.A. 1996: Evidence of Cretaceous(?) volcanism along the Churchill–Superior Boundary Zone, Manitoba (NTS 63G/4); *in Report of Activities 1996, Manitoba Energy and Mines, Minerals Division*, p. 122–126.
- Brady, A.E. and Moore, K.R. 2012: A mantle-derived dolomite silico-carbonatite from the southwest coast of Ireland; *Mineralogical Magazine*, v. 76, p. 357–376.
- Chakhmouradian, A.R., 2006: High-field-strength elements in carbonatitic rocks: geochemistry, crystal chemistry and significance for constraining the sources of carbonatites; *Chemical Geology*, v. 235, p. 138–160.
- Chakhmouradian, A.R. and Mitchell, R.H. 2000: Occurrence, compositional variation and alteration of perovskite in kimberlites; *Canadian Mineralogist*, v. 38, p. 975–994.
- Chakhmouradian, A.R. and Wall, F. 2012: Rare earth elements: minerals, mines, magnets (and more); *Elements*, v. 8, p. 333–340.
- Chakhmouradian, A.R., Böhm, C.O., Demény, A., Reguir, E.P., Hegner, E., Creaser, R.A., Halden, N.M. and Yang, P. 2009b: “Kimberlite” from Wekusko Lake, Manitoba: actually a diamond-indicator bearing dolomite carbonatite; *Lithos*, v. 112, p. 347–357.
- Chakhmouradian, A.R., Couëslan, C.G. and Reguir, E.P. 2009a: Evidence for carbonatite magmatism at Paint Lake, Manitoba (parts of NTS 63O8, 63P5, 12); *in Report of Activities 2009, Manitoba Science, Technology, Energy and Mines, Manitoba Geological Survey*, p. 118–126.
- Chakhmouradian, A.R., Mumin, A.H., Demény, A. and Elliott, B. 2008: Postorogenic carbonatites at Eden Lake, Trans-Hudson Orogen (northern Manitoba, Canada): geological setting, mineralogy and geochemistry; *Lithos*, v. 103, p. 503–526.
- Chakhmouradian, A.R., Reguir, E.P., Kamenetsky, V.S., Sharygin, V.V. and Golovin, A.V. 2013: Trace-element partitioning in perovskite: implications for the geochemistry of kimberlites and other mantle-derived undersaturated rocks; *Chemical Geology*, v. 353, p. 112–131.
- Chakhmouradian, A.R., Reguir, E.P., Kressall, R.D., Crozier, J., Pisiak, L.K., Sidhu, R. and Yang, P. 2015: Carbonatite-hosted niobium deposit at Aley, northern British Columbia (Canada): mineralogy, geochemistry and petrogenesis; *Ore Geology Reviews*, v. 64, p. 642–666.
- Chakhmouradian, A.R., Reguir, E.P. and Zaitsev, A.N. 2016: Calcite and dolomite in intrusive carbonatites. I. Textural variations; *Mineralogy and Petrology*, v. 110, p. 333–360.
- Couëslan, C.G. 2008: Preliminary results from geological mapping of the west-central Paint Lake area, Manitoba (parts of NTS 63O8, 9, 63P5, 12); *in Report of Activities 2008, Manitoba Science, Technology, Energy and Mines, Manitoba Geological Survey*, p. 99–108.
- Digonnet, S., Goulet, N., Bourne, J., Stevenson, R. and Archibald, D. 2000: Petrology of the Abloviak aillikite dykes, New Québec: evidence for a Cambrian diamondiferous alkaline province in north-eastern North America; *Canadian Journal of Earth Sciences*, v. 37, p. 517–533.
- Gilbert, H.P. and Bailes, A.H. 2005: Geology of the southern Wekusko Lake area, Manitoba (NTS 63J12NW); Manitoba Industry, Economic Development and Mines, Manitoba Geological Survey, Geoscientific Map MAP2005-2, scale 1:20 000.
- Hajnal, Z., Lewry, J., White, D., Ashton, K., Clowes, R., Stauffer, M., Gyorfi, I. and Takacs, E. 2005: The Sask Craton and Hearne Province margin: seismic reflection studies in the western Trans-Hudson Orogen; *Canadian Journal of Earth Sciences*, v. 42, p. 403–419.
- Hetman, C.M., Scott-Smith, B.H., Paul, J.L. and Winter, F. 2004: Geology of the Gahcho Kué kimberlite pipes, NWT, Canada: root to diatreme magmatic transition zones; *Lithos*, v. 76, p. 51–74.
- Kong, J.M., Boucher, D.R. and Scott-Smith, B.H. 1999: Exploration and geology of the Attawapiskat Kimberlites, James Bay Lowlands, northern Ontario, Canada; *in Proceedings of the VII<sup>th</sup> International Kimberlite Conference (Volume 1)*; Red Roof Design, Cape Town, South Africa, p. 452–467.
- Krasnova, N.I., Petrov, T.G., Balaganskaya, E.G., Garcia, D., Moutte, J., Zaitsev, A.N. and Wall, F. 2004: Introduction to phoscorites: occurrence, composition, nomenclature and petrogenesis; *in Phoscorites and Carbonatites from Mantle to Mine: The Key Example of the Kola Alkaline Province*, F. Wall and N. Zaitsev (ed.), Mineralogical Society of Great Britain and Ireland, London, p. 45–74.
- Lewry, J.F., and Collerson, K.D. 1990: Trans-Hudson Orogen: extent, subdivision, and problems, *in The Early Proterozoic Trans-Hudson Orogen of North America*, J.F. Lewry and M.R. Stauffer (ed.), Geological Association of Canada, Special Publication 37, p. 1–14.
- Lucas, S.B., Stern, R.A., Syme, E.C., Reilly, B.A. and Thomas, D.J. 1996: Intraoceanic tectonics and the development of continental crust: 1.92–1.84 Ga evolution of the Flin Flon Belt, Canada; *Geological Society of America Bulletin*, v. 108, p. 602–629.
- McDonough, W.F. and Sun, S.-s. 1995: The composition of the Earth; *Chemical Geology*, v. 120, p. 223–253.
- Mitchell, R.H. 1983: The Ile Bizard intrusion, Montreal, Quebec – kimberlite or lamprophyre? Discussion; *Canadian Journal of Earth Sciences*, v. 20, p. 1493–1496.
- Mitchell, R.H. 1986: *Kimberlites: Mineralogy, Geochemistry and Petrology*; Plenum, New York, New York, 442 p.
- Mitchell, R.H. 1995: *Kimberlites, Orangeites, and Related Rocks*; Plenum, New York, New York, 410 p.
- Mitchell, R.H., Scott-Smith, B.H. and Larsen, L.M. 1999: Mineralogy of ultramafic dikes from the Sarfartoq, Sisimiut and Maniitsoq areas, West Greenland; *in Proceedings of the VII<sup>th</sup> International Kimberlite Conference*; Red Roof Design, Cape Town, South Africa, p. 574–583.
- Mumin, A.H. 2002: Discovery of a carbonatite complex at Eden Lake (NTS 64C9), Manitoba, *in Report of Activities 2002, Manitoba Industry, Trade and Mines, Manitoba Geological Survey*, p. 187–197.
- NATMAP Shield Margin Project Working Group 1998: *Geology, NATMAP Shield Margin Project area, Flin Flon belt, Manitoba/Saskatchewan*; Geological Survey of Canada, Map 1968A, scale 1:100 000.
- Raeside, R.P. and Helmstaedt, H. 1982: The Ile Bizard intrusion, Montreal, Quebec – kimberlite or lamprophyre? *Canadian Journal of Earth Sciences*, v. 19, p. 1996–2011.

- Reguir, E.P., Camacho, A., Yang, P., Chakhmouradian, A.R., Kamenetsky, V.S. and Halden, N.M. 2010: Trace-element study and uranium-lead dating of perovskite from the Afrikanda plutonic complex, Kola Peninsula (Russia) using LA-ICP-MS; *Mineralogy and Petrology*, v. 100, p. 95–103.
- Reguir, E.P., Chakhmouradian, A.R., Halden, N.M., Malkovets, V.G. and Yang, P. 2009: Major- and trace-element compositional variation of phlogopite from kimberlites and carbonatites as a petrogenetic indicator; *Lithos*, v. 112S, p. 372–384.
- Reid, K.D. and Gagné, S. 2016: Examination of exploration drillcore from the south Wekusko Lake area, eastern Flin Flon belt, north-central Manitoba (parts of NTS 63J5, 12, 63K8, 9); *in* Report of Activities 2016, Manitoba Growth Enterprise and Trade, Manitoba Geological Survey, p. 74–86.
- Skinner, E.M.W. and Marsh, J.S. 2004: Distinct kimberlite pipe classes with contrasting eruption processes; *Lithos*, v. 76, p. 183–200.
- Smith, M.P., Campbell, L.S. and Kynicky, J. 2015: A review of the genesis of the world class Bayan Obo Fe-REE-Nb deposits, Inner Mongolia, China: multistage processes and outstanding questions; *Ore Geology Reviews*, v. 64, p. 459–476.
- Syme, E.C., Lucas, S.B., Bailes, A.H. and Stern, R.A. 1999: Contrasting arc and MORB-like assemblages in the Paleoproterozoic Flin Flon Belt, Manitoba, and the role of intra-arc extension in localizing volcanic-hosted massive sulphide deposits; *Canadian Journal of Earth Sciences*, v. 36, p. 1767–1788.
- Tappe, S., Foley, S.F., Jenner, J.A., Heaman, L.M., Kjarsgaard, B.A., Romers, R.L., Stracke, A., Joyces, N. and Hoefs, J. 2006: Genesis of ultramafic lamprophyres and carbonatites at Aillik Bay, Labrador: a consequence of incipient lithospheric thinning beneath the North Atlantic craton; *Journal of Petrology*, v. 47, p. 1261–1315.
- Tappe, S., Steenfelt, A., Heaman, L.M. and Simonetti, A. 2009: The newly discovered Jurassic Tikiusaaq carbonatite-aillikite occurrence, West Greenland, and some remarks on carbonatite-kimberlite relationships; *Lithos*, v. 112S, p. 385–399.
- Wyatt, B.A., Baumgartner, M., Anckar, E and Grutter, H., 2004: Compositional classification of “kimberlitic” and “non-kimberlitic” ilmenite; *Lithos*, v. 77, p. 819–840.
- Xu, C., Kynicky, J., Chakhmouradian, A.R., Qi, L. and Song, W. 2010: A unique Mo deposit associated with carbonatites in the Qinling orogenic belt, central China; *Lithos*, v. 118, p. 50–60.
- Zurevinski, S.E. and Mitchell, R.H. 2011: Highly evolved hypabyssal kimberlite sills from Wemindji, Quebec, Canada: insights into the process of flow differentiation in kimberlite magmas; *Contributions to Mineralogy and Petrology*, v. 161, p. 765–776.
- Zwanzig, H.V. and Bailes, A.H. 2010: Geology and geochemical evolution of the northern Flin Flon and southern Kisseynew domains, Kisseynew–File Lake areas, Manitoba (parts of NTS 63K, N); Manitoba Growth, Enterprise and Trade, Manitoba Geological Survey, Geoscientific Report GR2010-1, 134 p.